Indian Journal of Chemistry
Vol. 60A, July 2021, pp. 932-937

Highly dispersed and ultrafine Co_3O_4@N-doped carbon catalyst derived from metal-organic framework for efficient oxygen reduction reaction

Yuanyuan Chu[a,b,*], Bohan Deng[a,b], Kuixiao Wang[a,b], Yu Xue[a,b] & Xiaoyao Tan[a,b]

[a]State Key Laboratory of Separation Membranes & Membrane Processes, [b]School of Chemistry & Chemical Engineering, Tiangong University, No.399 Binshui West Road, Tianjin 300387, China

*E-mail: chuyuanyuan@tiangong.edu.cn

Received 05 February 2021; Revised and accepted 07 April 2021

Electrocatalysts are composed of transition metal/metal oxide and N-doped carbon can overcome the sluggish kinetics of oxygen reduction reactio. Herein, the Co_3O_4/ketjen black (KB)@MOF-derived with uniformly dispersed and ultrafine Co_3O_4 nanoparticles (1-5 nm) are synthesized by a facile in-situ method and subsequent mild pyrolysis process. It exhibits enhanced activity with onset potential of 0.96 V (vs. RHE) and a half-wave potential of 0.86 V (vs. RHE) in 0.1 M KOH solution, the excellent durability with $E_{1/2}$ a small negative shift of 10 mV after 5000 continuous cycles and good methanol-tolerance property. The ultrahigh catalytic performance of Co_3O_4/KB@MOF-derived can be ascribed to the small particle size range of 1-5 nm of Co_3O_4, as well as the strong interaction between the *in-situ* formed N-Co_3O_4 active sites and substrate under the mild calcination temperature. Above all, these indicate that the as-prepared Co_3O_4/KB@MOF-derived may be a good alternative to commercial Pt-based catalysts.

Keywords: Co_3O_4/KB@MOF-derived, Durability, Methanol-tolerance, Oxygen reduction reaction, Direct methanol fuel cell

Direct methanol fuel cells (DMFCs) are highly expected to be the future energy technology for transport and portable equipment due to its high energy conversion efficiency, flexible and convenient manipulation[1]. Oxygen reduction reaction (ORR) plays a vital role in DMFCs. Currently, Pt-based[2] catalysts act as the best catalysts for ORR, however, the wide-ranging application of Pt is bound to the instability and high price and accordingly it is extremely desirable to design low-cost non-noble metal or metal-free catalyst with good ORR catalytic activity and high stability[3]. For the past few years, transition-metal oxides with carbon composites such as N-TiO_2/NG[4], α-MnO_2/C[5], Ag-Co_3O_4@NC/CNT[6] etc. have attracted great interests as Pt alternatives for ORR. Typically, the spinel type Co_3O_4 is a promising ORR electrocatalyst in alkaline owing to the unique structure[7-9]. It is known that the catalytic activities of the Co_3O_4 materials were influenced by its size, distribution and morphology, as well as their electron transfer properties[10]. Recently, various approaches have been used to synthesize Co_3O_4 nanoparticles by controlling the particle size and improving the dispersion of the catalyst. For example, many studies have reported that Co_3O_4 particles were supported on porous carbon nanomaterials, which have large specific surface[11,12]. However, the spontaneous aggregation of Co_3O_4 particles is still unsolved mainly due to the high calcination temperature leading to the agglomeration of metal oxide particles or a growing particle size[13]. Therefore, introducing proper support, in-situ synthesizing the Co_3O_4 nanoparticles at relatively mild condition to inhibit the aggregation, enhance the interaction between active sites and support deserves to be strongly pursued, toward meeting our goal of making efficient ORR electrocatalysts with good catalytic reactivity and high structural stability[14].

Zeolitic imidazolate frameworks (ZIFs) own an accessible large surface area, porous structure, and thermal and chemical stabilities, emerging as a novel templates in the synthesis of metal-based[15], metal-oxide-based[16] or carbon-based[17] nanomaterials for ORR. For example, Liu *et al.*[18] prepared NC@Co-NGC catalyst with double-shelled hybrid nanocages using ZIF-67@ZIF-8 as template and calcined at 800 °C, which showed superior activities with the onset potential (E_{onset}) and half-wave potentials ($E_{1/2}$) of 0.92 V and 0.82 V, respectively. Wang *et al.*[19] prepared encapsulated Co_3O_4 catalyst by pyrolyzing ZIF-67 at 800 °C and demonstrated the superior E_{onset} of 0.918 V. Despite the good performances have been

achieved by these catalysts for ORR, they still need to be further improved for real application. It is generally considered that the high temperature pyrolysis (above 700 °C) play a vital role in the production of active sites, but it is inevitable caused the agglomeration and growth of particle size, and the reconstruction of carbon structure and thus the active sites are lost, which is one of the root reasons for unsatisfied performance[13,20]. Therefore, it is desirable to control the particle size and increase the active sites through proper strategies, study the relationship between the interaction between active sites and support and its corresponding catalytic stability.

In this study, we report an easy method that adopts in-situ assembling Co-ZIF-67 on ketjen black (KB) followed by calcination at a mild temperature (500 °C) to produce the Co_3O_4/KB @MOF-derived electrocatalyst, which effectively promotes the formation of active sites and prevents the agglomeration of Co_3O_4 particles[21]. It is found that the abundant N-Co_3O_4 active sites with small particle size exhibit excellent activity and good stability for ORR in alkaline media.

Materials and Methods

Preparation of ZIF-67@KB & Co_3O_4/KB@MOF-derived catalysts

For ZIF-67@KB catalyst, firstly, 40 mg of KB (EC-600JD, Akzonobel Supplier, Japan) were dispersed in 30 mL absolute methanol by sonication. 345 mg 2-methylimidazole powder was added under vigorous stirring. 30 min later, 5 mL of a 0.2 M $Co(NO_3)_2$ methanol solution was injected into the mixture. The reaction was continues for 3 h. Finally, the products were purified by centrifugation, washed three times with methanol and dried at 60 °C in vacuum for 12 h for further application. For Co_3O_4/KB@MOF-derived catalyst, the as prepared ZIF-67@KB electrocatalyst were annealed at 500 °C for 1 h at the heating rate of 5 °C min^{-1} in N_2 atmosphere.

Characterization

Structural characterization

X-ray diffraction (XRD) data of the catalysts were collected from D/max-B diffractometer (Japan) using a Cu Kα X-ray source. Scanning electron microscopy (SEM) images were taken on a Leo 1530 field-emission scanning electron microscope and transmission electron microscope (TEM) images were recorded using TECNAI G2 F30 instrument. The structure of samples was measured by a XploRA PLUS Raman spectrometer with excitation by 638 nm laser light. X-ray photoelectron spectroscopy (XPS) was used to determine the chemical state and elemental analysis with PHI model 5700.

Electrochemical activity characterization

All tests were conducted at room temperature of 25 °C using CHI 760E with a three-electrode system. The graphite rod as the counter electrode, Hg/HgO as the reference electrode, and the prepared glassy carbon (GC) electrode (diameter = 5 mm) was used as working electrode. 6 mg catalyst, 0.5 mL ethanol, 0.5 mL water and 50 µL Nafion (5 wt%) were added into a vial, ultrasounded for half an hour and then 10 µL of the ultrasonic catalyst ink was applied to the working electrode, and waited half an hour for the ink to air-dry. The above three electrodes and a 0.1 M KOH solution were used to form a three-electrode system for electrochemical measurements. Cyclic voltammetry (CV) tests were carried out in N_2 and O_2 saturated electrolytes. Linear sweep voltammetry (LSV) tests were performed at a rotating rate varying from 400 to 2000 rpm. To check CH_3OH tolerance of the prepared samples, the concentration of 20000 ppm methanol was added to the electrolyte, and another LSV test was performed at 1600 rpm. LSV curves were compensated by *iR* (current × internal resistance). The transferred electron numbers per O_2 and kinetic current density in the ORR were determined by the Koutechy-Levich (K-L) equation[22,23] as follows.

$$\frac{1}{J} = \frac{1}{J_K} + \frac{1}{B\omega^{1/2}} \quad \ldots(1)$$

$$B = 0.62nFC_0D_0^{2/3}\upsilon^{-1/6} \quad \ldots(2)$$

Where, J is the measured current density and J_k is the kinetic current density and ω is the electrode rotating speed in rpm, n represents the overall number of electrons gained per O_2, F = 96485 C mol^{-1} (Faraday constant), C_0 = 1.1×10^{-3} mol L^{-3} (concentration of O_2), D_0 = 1.9×10^{-5} cm^2 s^{-1} (diffusion coefficient of O_2 in 0.1 M KOH), υ = 0.01 cm^2 s^{-1} (kinetic viscosity of the electrolyte).

Results and Discussion

Fig. 1 represents an ideal schematic synthesis process of Co_3O_4/KB@MOF-derived catalyst. The cobalt ion is trapped into the ZIF-67 framework and the sequent mild pyrolysis lead to the formation of

ultrafine Co_3O_4 nanoparticles in-situ supported on well-developed porous carbon structure.

Most Co-ZIF-67 frameworks were successfully combined with KB as depicted in Supplementary Data, Fig. S1. The subsequent pyrolysis of ZIF-67@KB at 500 °C is crucial for in-situ formation of N-Co_3O_4 active sites and well keep the Co-ZIF-67 framework morphology (Fig. 2a). The HRTEM and STEM images are shown in Fig. 2b and 2c, the Co_3O_4 nanoparticles evenly disperse with the small particle size (1-5 nm), and the apparent spacing of the lattice fringe of Co_3O_4 (220) and (311) measured from HRTEM are 0.286 nm and 0.25 nm, respectively, identifying the existence of Co_3O_4[24]. The element mapping images in Fig. 2d show the distribution of the elements of C (blue), O (yellow) and N (red) in Co_3O_4/KB@MOF-derived catalyst and of Co (green) in Co_3O_4 nanoparticles.

The XRD characteristic peaks of ZIF-67 (Fig. 3a) in Co_3O_4/KB@MOF-derived in Fig. 3b are partially disappeared, moreover, two weak characteristic peaks (220) and (311) of Co_3O_4 appear at 31.8° and 37.5°, indicating that the material in ZIF-67 is converted to Co_3O_4 during mild pyrolysis[21]. The (002) diffraction peak of carbon emerged at 23°, and as the Raman spectra of Co_3O_4/KB@MOF-derived catalyst shown in Supplementary Data, Fig. S2, the relative scale of the D to G band (I_D/I_G) is 1.46, indicating the excellent graphitization degree in Co_3O_4/KB @MOF-derived catalyst.

XPS characterization was performed to further analyze the chemical state and structure of Co_3O_4/KB@MOF-derived catalyst. Four distinct peaks of 803.5 eV, 798.1 eV, 785.8 eV and 781 eV can be seen in Fig. 4a, corresponding to the Co $2p_{1/2}$ and Co $2p_{3/2}$ spin orbit peaks of Co_3O_4[25]. The C 1s spectrum was presented in Fig. 4b, the four fitted peaks located at 284.6 eV, 285.5 eV, 286.5 eV and 288.5 eV are ascribed to graphitic layers (C-C/C=C), C=N, C-O and C=O, respectively[8]. The formation of

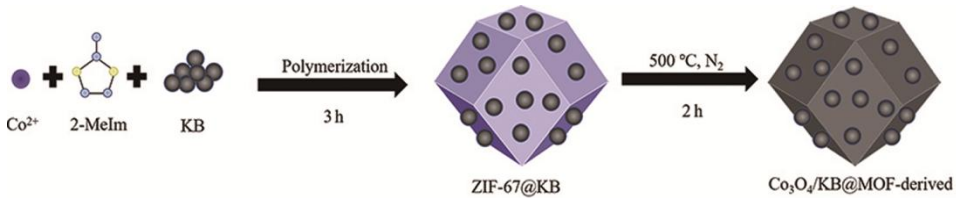

Fig. 1 — An ideal schematic synthesis process of Co_3O_4/KB@MOF-derived catalyst

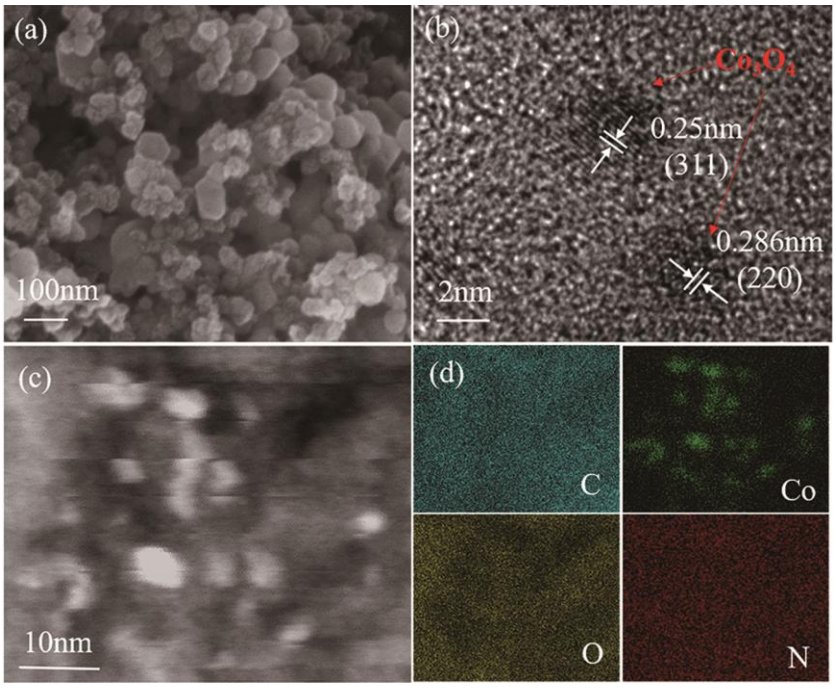

Fig. 2 — (a) SEM, (b) HRTEM, (c) STEM and (d) corresponding element mapping images of C, Co, O, N for Co_3O_4/KB@MOF-derived catalyst

C-O bonds was probably due to the formation of edge carbons with unpaired electrons by calcination. These marginal carbon atoms have unsaturated chemical bonds which can react with O_2 to form surface groups. The N 1s spectrum in Fig. 4c shows the four fitted peaks located at 398.3 eV, 399.2 eV, 400.2 eV and 401 eV, which are ascribed to pyridinic-N, Co-N, pyrrolic-N and graphitic-N, respectively. The emergence of Co-N suggested that the N-doped in Co_3O_4 phase successfully[26]. Co-N and pyridinic-N are the important reasons for the high performance for ORR catalyst of Co_3O_4/KB@MOF-derived catalyst[27]. A weak peak at 530.2 eV in O 1s spectrum is associated with the lattice oxygen of Co_3O_4 phase. The peak at 531.1 eV and 533.2 eV are ascribed to the vacancy oxygen of Co_3O_4 and the adsorbent oxygen species, which are conducive to improve the electron transfer efficiency and catalytic activity[28-30] (Fig. 4d).

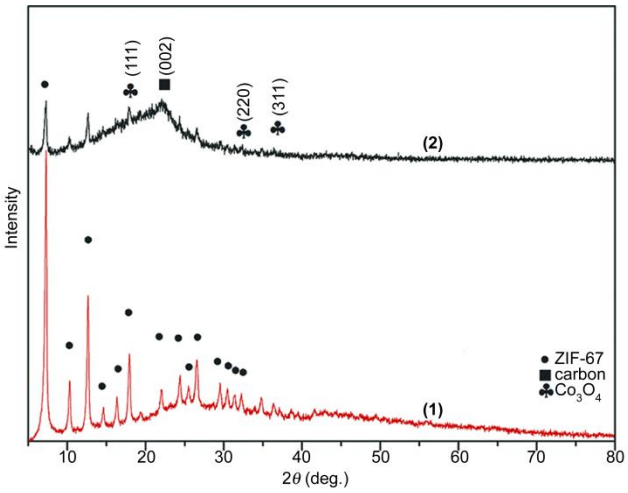

Fig. 3 — XRD patterns of ZIF-67@KB (1) and Co_3O_4/KB@MOF-derived (2) catalyst

The cathodic peak appears at 0.88 V in the 0.1 M KOH solution saturated with O_2 in Fig. 5a, indicating that the Co_3O_4/KB@MOF-derived shows activity for ORR. Surprisingly, it exhibits ultrahigh activity with an E_{onset} of 0.96 V and an $E_{1/2}$ of 0.86 V as shown in Fig. 5b, approaching to the performance of 20% Pt/C. However, the Co_3O_4/KB@MOF-derived displays lower Tafel slope (50.8 mV decade^{-1}) than that of 20% Pt/C (67.6 mV decade^{-1}), which can be believed that it displays better kinetic behaviour for ORR. The K-L curves of Co_3O_4/KB@MOF-derived shown in Fig. 5c to identify the ORR electron-transfer mechanism of catalyst, illustrates the first order reaction kinetics with respect to the amount of dissolved oxygen and a potential-independent electron transfer number (n). The calculated 'n' of Co_3O_4/KB@MOF-derived in Fig. 5d is 3.80, suggesting that it is a 4e$^-$ ORR pathway. Notably, the methanol tolerance of Co_3O_4/KB@MOF-derived is superior to that of commercial 20% Pt/C (Fig. 5e). Furthermore, the excellent electrocatalytic durability

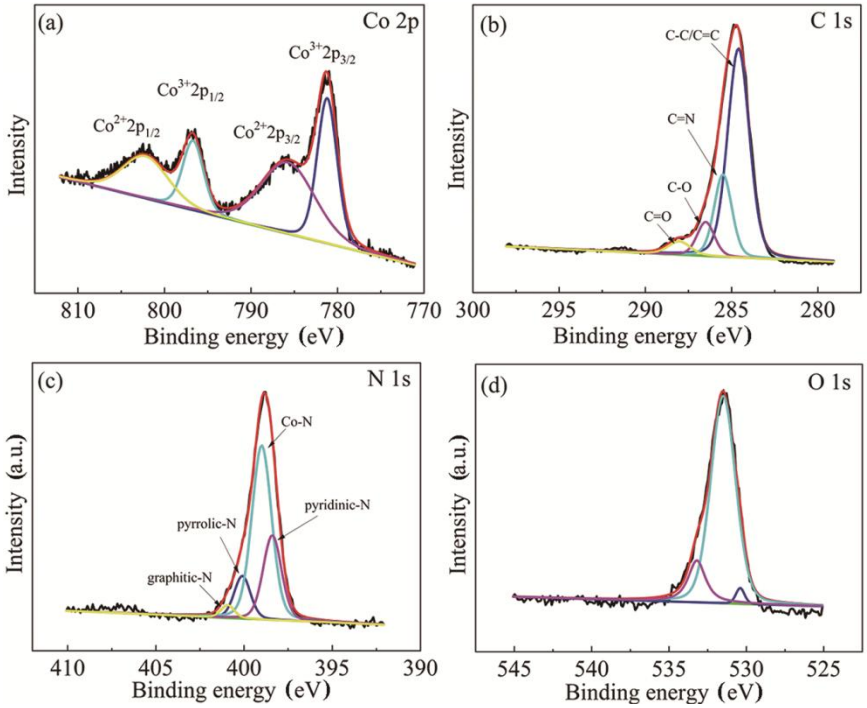

Fig. 4 — (a) Co 2p, (b) C 1s, (c) N 1s and (d) O 1s spectra of Co_3O_4/KB@MOF-derived catalyst

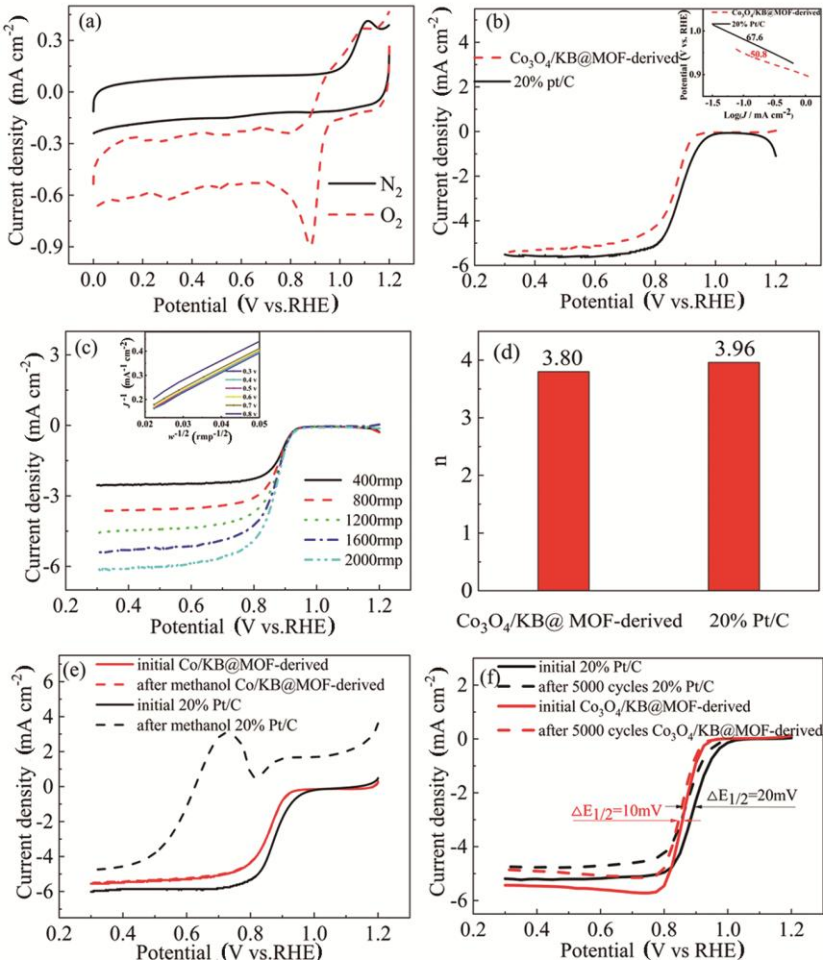

Fig. 5 — (a) CV, (b) LSV curves (Tafel curves in the inset), (c) LSV curves at different rates and the K-L plots range 0.3-0.8 V (inset), (d) Electron transfer number histogram, (e) LSV curves with and without CH3OH and (f) LSV curves before and after 5000 cycles

is achieved on Co_3O_4/KB@MOF-derived catalyst, as confirmed by continuous ageing test in Fig. 5f, which reveals that the $E_{1/2}$ of Co_3O_4/KB@MOF-derived catalyst only negatively shifted 10 mV after 5000 continuous cycles, significantly smaller than that of 20% Pt/C with 20 mV. The performances of Co_3O_4/KB@MOF-derived catalysts synthesized by pyrolysis under different temperatures are also compared in Supplementary Data, Fig. S3. The catalysts calcined at 500 °C demonstrated the optimum activity for ORR. The higher temperature (700 °C and 900 °C) caused a decline of ORR performance probably due to the agglomeration and growth of particle size, as well as the gasification of carbon and thus the active sites lost.

Conclusions

To sum up, the Co_3O_4/KB@MOF-derived catalyst with small particle size is synthesized and the small Co_3O_4 nanoparticles under the mild pyrolysis condition employing the well-developed MOF framework as template. The as-prepared catalyst exhibited outstanding activity with an E_{onset} of 0.96 V and an $E_{1/2}$ of 0.86 V (vs RHE) in 0.1 M KOH solution. After 5000 continuous cycles, the $E_{1/2}$ of Co_3O_4/KB@MOF-derived catalyst only negatively shifts 10 mV, indicating the superior durability. The Co_3O_4/KB@MOF-derived catalyst also exhibits the excellent methanol tolerance, which is superior to that of commercial 20% Pt/C. The good performance of the catalyst is ascribed to the mild pyrolysis condition which is benefit for the formation of small particle size of Co_3O_4 nanoparticle, as well as the abundant released active sites of N-Co_3O_4 and strong interaction between in-situ formed N-Co_3O_4 active sites and substrate responsible for the improvement of ORR activity in alkaline medium. Above all, the as-prepared Co_3O_4/KB@MOF-derived with excellent

activity and stability may be an alternative to commercial Pt-based catalysts.

Supplementary Data

Supplementary data associated with this article are available in the electronic form at http://nopr.niscair.res.in/jinfo/ijca/IJCA_60A(07)932-937_SupplData.pdf.

Acknowledgement

This work was supported by the National Natural Science Foundation of China (Grant No. 21206124 and 17JCQNJC06500).

References

1 Neburchilov V, Martin J, Wang H & Zhang J, *J Power Sources*, 169 (2007) 221.
2 Rao C V, Singh S K & Viswanathan B, *Indian J Chem*, 47A (2008) 1619.
3 Hu C & Dai L, *Adv Mater*, 29 (2017) 1604942.
4 Yuan W, Li J, Wang L, Chen P, Xie A & Shen Y, *ACS Appl Mater Interfaces*, 6 (2014) 21978.
5 Majidi M R, Shahbazi F, Hosseini M & Ahadzadeh I, *Bioelectrochemistry*, 125 (2019) 38.
6 Jiang M, He H, Yi W J, Huang W, Pan X, Wang M Y & Chao Z S, *Electrochem Commun*, 77 (2017) 5.
7 Xu J, Gao P & Zhao T, *Energy Environ Sci*, 5 (2012) 5333.
8 Jing H, Song X, Ren S, Shi Y, An Y, Yang Y, Feng M, Ma S & Hao C, *Electrochim Acta*, 213 (2016) 252.
9 Hamdani M, Singh R N & Chartier P, *Int J Electrochem Sci*, 5 (2010) 556.
10 Mu J, Zhang L, Zhao M & Wang Y, *ACS Appl Mater Interfaces*, 6 (2014) 7090.
11 Wang Z, Zhang X, Liu X, Lv M, Yang K & Meng J, *Carbon*, 49 (2011) 161.
12 Wang Z, Xu W, Chen X, Peng Y, Song Y, Lv C, Liu H, Sun J, Yuan D, Li X, Guo X, Yang D & Zhang L, *Adv Funct Mater*, 29 (2019) 1902875.
13 Li J, Zhang H, Samarakoon W, Shan W, Cullen D A, Karakalos S, Chen M, Gu D, More K L, Wang G, Feng Z, Wang Z & Wu G, *Angew Chem Int Edit*, 58 (2019) 18971.
14 Bao L, Li T, Chen S, Peng C, Li L, Xu Q, Chen Y, Ou E & Xu W, *Small*, 13 (2017) 1602077.
15 Guo J, Gadipelli S, Yang Y, Li Z, Lu Y, Brett D J L & Guo Z, *Inorg Chem*, 54 (2014) 9483.
16 Huang M, Zhang Y, Li F, Zhang L, Wen Z & Liu Q, *Joule*, 2 (2018) 1242.
17 Varghese B, Teo C H, Zhu Y , Reddy M V, Chowdari B V R, Wee A T S, Tan V B C, Lim C T & Sow C H, *Adv Mater*, 31 (2019) 1804799.
18 Xu L, Zou Y, Xiao Z & Wang S, *Adv Mater*,29 (2017) 1700874.
19 Dou S, Li X, Tao L, Huo J & Wang S,*Chemi Commun*,52 (2016) 9727.
20 Shao Y, Dodelet J P, Wu G & Zelenay P, *Adv Mater*, 31 (2019) 1807615.
21 Guo J, Gadipelli S, Yang Y, Li Z, Lu Y, Brett D J L & Guo Z, *J Mater Chem A*, 7 (2019) 3544.
22 Liang Y, Zhou J, Li Y, Wang J, Regier T & Dai H, *J Am Chem Soc*, 134 (2012) 3517.
23 Xiong W, Liu Y, Ramakrishnan T S, Dai L & Jiang L, *J Am Chem Soc*, 132 (2010) 15839.
24 Huang M, Zhang Y, Li F, Zhang L, Wen Z &Liu Q, *J Power Sources*, 252 (2014) 98.
25 Varghese B, Teo C H, Zhu Y, Reddy M V, Chowdari B V R, Wee A T S, Tan B V C, Lim C T & Sow C H, *Adv Funct Mater*, 17 (2007) 1932.
26 Xu L, Zou Y, Xiao Z & Wang S, *J Energy Chem*, 35 (2019) 24.
27 Wang X,Liu J &Liu Z, *Adv Mater*, 30 (2018) 1800005.
28 Xiong S, Yuan C, Zhang X, Xi B & Qian Y, *Chemistry*, 15 (2009) 5320.
29 Petitto S C, Marsh E M, Carson G A & Langell M A, *J Mol Catal A: Chem*, 281 (2008) 49.
30 Lu Y, Zhan W, He Y, Wang Y, Kong X, Kuang Q, Xie Z& Zheng L, *ACS Appl Mater Interfaces*, 6 (2014) 4186.